

# Reassessment of sst<sub>3</sub> Somatostatin Receptor Expression in Human Normal and Neoplastic Tissues Using the Novel Rabbit Monoclonal Antibody UMB-5

Amelie Lupp<sup>a</sup> Falko Nagel<sup>a</sup> Christian Doll<sup>a</sup> Christoph Röcken<sup>b</sup>  
Matthias Evert<sup>c</sup> Christian Mawrin<sup>d</sup> Wolfgang Saeger<sup>e</sup> Stefan Schulz<sup>a</sup>

<sup>a</sup>Department of Pharmacology and Toxicology, University Hospital, Friedrich Schiller University Jena, Jena, <sup>b</sup>Department of Pathology, Christian Albrechts University, Kiel, <sup>c</sup>Department of Pathology, Ernst Moritz Arndt University Greifswald, Greifswald, <sup>d</sup>Department of Neuropathology, Otto von Guericke University Magdeburg, Magdeburg, and <sup>e</sup>Department of Pathology, Marienkrankenhaus Hamburg, Hamburg, Germany

## Key Words

Neuroendocrine tumors · Somatostatin · Antibody · Somatostatin receptor · Pituitary

## Abstract

**Background:** Among the five somatostatin receptors (sst<sub>1</sub>–sst<sub>5</sub>), the sst<sub>3</sub> receptor displays a distinct pharmacological profile. Like sst<sub>2</sub>, the sst<sub>3</sub> receptor efficiently internalizes radiolabeled somatostatin analogs. Unlike sst<sub>2</sub>, however, internalized sst<sub>3</sub> receptors are rapidly transferred to lysosomes for degradation. Apart from this, very little is known about the clinical relevance of the sst<sub>3</sub> receptor, which may in part be due to the lack of specific monoclonal sst<sub>3</sub> antibodies. **Methods:** Here, we have extensively characterized the novel rabbit monoclonal anti-human sst<sub>3</sub> antibody UMB-5 using transfected cells and receptor-expressing tissues. UMB-5 was then subjected to immunohistochemical staining of a series of 190 formalin-fixed, paraffin-embedded normal and neoplastic human tissues. **Results:** Specificity of UMB-5 was demonstrated by detection of a broad band migrating at a

molecular weight of 70,000–85,000 in immunoblots from human pituitary. After enzymatic deglycosylation, the size of this band decreased to a molecular weight of 45,000. Tissue immunostaining was completely abolished by pre-adsorption of UMB-5 with its immunizing peptide. In addition, UMB-5 detected distinct cell populations in human tissues like pancreatic islets, anterior pituitary, adrenal cortex, adrenal medulla, and enteric ganglia, similar to that seen with a rabbit polyclonal antibody generated against a different carboxyl-terminal epitope of the sst<sub>3</sub> receptor. In a comparative immunohistochemical study, UMB-5 yielded predominant plasma membrane staining in the majority of pituitary adenomas, pheochromocytomas, and a subset of neuroendocrine tumors. The sst<sub>3</sub> receptor was also present in many glioblastomas, pancreatic, breast, cervix, and ovarian carcinomas. **Conclusion:** The rabbit monoclonal antibody UMB-5 may prove of great value in the identification of sst<sub>3</sub>-expressing tumors during routine histopathological examinations. Given its unique trafficking properties, these tumors may be potential candidates for sst<sub>3</sub>-directed receptor radiotherapy.

Copyright © 2012 S. Karger AG, Basel

## Introduction

Somatostatin is a cyclic neuropeptide that inhibits the secretion of a large number of hormones from the anterior pituitary, pancreas, and endocrine cells within the gastrointestinal tract, regulates neurotransmission both in the brain and in the peripheral nervous system, and exerts antiproliferative effects. Additionally, it causes a reduction of gastrointestinal tract motility and gallbladder contractility and plays a regulatory role in the immune system [1–3]. The biological functions of somatostatin are mediated via a family of G-protein-coupled receptors, *sst*<sub>1</sub> to *sst*<sub>5</sub>. For *sst*<sub>2</sub> two splice variants have been identified in rodents, the unspliced *sst*<sub>2A</sub> and the spliced *sst*<sub>2B</sub>, carrying a different carboxyl terminus. In a varying pattern and density, somatostatin receptors are present throughout the body, including brain, pituitary gland, neuroendocrine cells of the gastrointestinal tract and pancreas, thyroid gland, adrenals, and immune system [1–3]. Somatostatin receptors have also been found in many tumors, including pituitary adenomas and neuroendocrine tumors [4, 5], where they mediate inhibitory effects on both hormone secretion and tumor growth [6, 7]. Apart from the tissue distribution, *sst* receptors differ also in their pharmacological profile for synthetic somatostatin analogs, in their regulation of intracellular signaling pathways, and in their biological functions [8–10]. For the *sst*<sub>3</sub> receptor it has been shown that upon its activation apoptosis can be induced, which displays a unique function among the *sst* receptor family. Consequently, it has been reported that *sst*<sub>3</sub> stimulation results in an induction of two important pro-apoptotic proteins, p53 and Bax, as well as in a translocation of protein tyrosine phosphatase (PTP) to the plasma membrane [8, 11, 12]. On the other hand, it has been demonstrated that the activated *sst*<sub>3</sub> receptor mediates an inhibition of tumor angiogenesis and growth, via regulation of endothelial nitric oxide synthase (eNOS) and mitogen-activated protein kinase (MAPK) activities [13]. Thus, the *sst*<sub>3</sub> receptor is of considerable interest as a pharmacological target for tumor therapy. Additionally, the *sst*<sub>3</sub> receptor seems to be involved in the control of permeability and biogenesis of epithelial tight junctions and, as a consequence, in the regulation of paracellular conductance [14]. Also with respect to its regulation, the *sst*<sub>3</sub> receptor seems to be different from other members of the *sst* receptor family. Both human and rat *sst*<sub>3</sub> have been shown to internalize rapidly after agonist stimulation and subsequent phosphorylation at the carboxyl terminal tail through a  $\beta$ -arrestin-clathrin-dependent pathway. In contrast to the

*sst*<sub>2A</sub> receptor, however, only part of the internalized receptors are redistributed to the plasma membrane after agonist withdrawal. A large proportion of the receptor is sequestered into intracellular clusters of larger vesicles and degraded after multiple ubiquitination, thus leading to profound downregulation of the *sst*<sub>3</sub> receptor after sustained agonist stimulation [10, 15]. This may be the molecular basis for the observation that, after intravenous injection of radiolabeled *sst*<sub>2</sub>- or *sst*<sub>3</sub>-receptor ligands into mice bearing *sst*<sub>2</sub>- or *sst*<sub>3</sub>-expressing tumors, with a *sst*<sub>3</sub>-directed radioligand a much more pronounced and sustained uptake was observed than with a *sst*<sub>2</sub>-directed radioligand [16, 17]. Thus, the *sst*<sub>3</sub> receptor may be of particular interest as a target for receptor radiotherapy of human tumors.

However, in comparison to *sst*<sub>2</sub> and to *sst*<sub>5</sub> receptors, much less is known about the precise tissue distribution, downstream signaling, and function of the *sst*<sub>3</sub> receptor. This may be in part due to the lack of suitable monoclonal antibodies, available in sufficient amounts for immunohistochemical staining of formalin-fixed, paraffin-embedded human tissue samples obtained during routine histopathological preparations.

Recently, we have extensively characterized two novel rabbit monoclonal antibodies against the *sst*<sub>2A</sub> receptor and against the human *sst*<sub>5</sub> receptor named UMB-1 and UMB-4, respectively. We have shown that both antibodies selectively detect their cognate receptor in crude membrane extracts from *sst* receptor-expressing cells and tissues and that they are excellently suited for the assessment of *sst*<sub>2A</sub> or *sst*<sub>5</sub> expression in fixed human tissue samples [18–20]. Given the numerous advantages of a rabbit monoclonal antibody compared with the currently available polyclonal anti-human *sst*<sub>3</sub> antisera, we have now generated and thoroughly characterized a rabbit monoclonal antibody directed against the carboxyl-terminal tail of the human *sst*<sub>3</sub> receptor. We have then used the novel antibody UMB-5 to evaluate the prevalence and cellular localization of *sst*<sub>3</sub> in a large series of formalin-fixed, paraffin-embedded human normal and neoplastic tissue samples.

## Materials and Methods

### *Tissue Specimens for Immunohistochemistry*

A total of 190 human tumor specimens were obtained from the Departments of Pathology of the Charité Universitätsmedizin Berlin, Ernst Moritz Arndt University Greifswald, Otto von Guericke University Magdeburg, and Marienkrankenhaus Hamburg, Germany. Permission was obtained from the local ethics commit-

tees to access material from the pathology archives. The following tumor species were investigated: pituitary adenoma (n = 41, classified as non-functioning adenoma [n = 6], ACTH-producing adenoma [n = 8], and GH-producing adenoma [n = 27]), glioblastoma (n = 6), pancreatic adenocarcinoma (n = 10), renal clear cell carcinoma (n = 9), pheochromocytoma (n = 13), neuroendocrine tumors of the lung (n = 2), of the gut (n = 31), and pancreatic insulinoma (n = 5) as well as lymph node metastases (n = 16) and liver metastases (n = 13) from neuroendocrine tumors, prostate adenocarcinoma (n = 9), breast carcinoma (n = 12, classified as invasive ductal carcinoma [n = 8], invasive lobular carcinoma [n = 2], and solid neuroendocrine carcinoma of the breast [n = 2]), cervix carcinoma (n = 11, classified as squamous cell carcinoma [n = 7], adenocarcinoma [n = 3], and neuroendocrine tumor [n = 1]), and ovarian tumors (n = 12, classified as serous-papillary ovarian adenocarcinoma [n = 5], granulosa cell tumor [n = 4], rhabdomyosarcoma [n = 2], and Brenner tumor [n = 1]). Many of the tumor specimens contained adjacent non-malignant tissue, which enabled us to analyze the distribution of sst<sub>3</sub> in normal tissues as well. Additionally, tumor-free human tissue samples from pituitary, liver, pancreas, kidney, and different parts of the gut were also evaluated and the staining patterns compared to those seen in the tissues surrounding, e.g., renal clear cell carcinoma or neuroendocrine tumors and their metastases. In no case, differences were observed. All tissue specimens had been fixed in formalin and embedded in paraffin. In addition, pituitary samples from human autopsy were obtained from the Department of Neuropathology, Otto von Guericke University Magdeburg, Germany. Samples were frozen in liquid nitrogen and stored at -80°C until Western blot analysis.

#### *Antibodies*

The rabbit monoclonal antibody UMB-5 was generated against the carboxyl-terminal tail of the human sst<sub>3</sub> and custom produced by Epitomics (Burlingame, Calif., USA). The identity of the peptide used for immunizations of the rabbits was QLLPQEASTGKESSTMRISYL, which corresponds to the residues 398–418 of the human sst<sub>3</sub> receptor. This sequence is unique for the human sst<sub>3</sub> receptor. Consequently, UMB-5 does not cross-react with rat or mouse sst<sub>3</sub> receptors. The peptide was purified and coupled to keyhole limpet hemocyanin. The conjugate was mixed 1:1 with Freund's adjuvant and injected into four rabbits for antiserum production. Injection was performed at 4-week intervals, and serum was obtained from the second injection on. The specificity of the antisera was initially tested using Dot blot analysis. At the optimal time point of antibody production, the animals were sacrificed and rabbit hybridoma cells were produced by fusing B-cells from the spleen with myeloma cells.

The immunohistochemical staining pattern of UMB-5 was compared to that of the affinity-purified rabbit polyclonal anti-human sst<sub>3</sub> antibody {4823}, which is directed to a different epitope, QERPPSRVA, corresponding to the residues 385–393 of the human sst<sub>3</sub> receptor. These residues are located in close proximity to the carboxyl terminus of human sst<sub>3</sub> (fig. 1). For comparison of the expression patterns, adjacent sections of the pituitary adenoma samples were also stained with the rabbit monoclonal anti-sst<sub>2A</sub> antibody UMB-1 or the rabbit monoclonal anti-human sst<sub>5</sub> antibody UMB-4. The polyclonal antibody {4823} as well as the monoclonal antibodies UMB-1 and UMB-4 have been extensively characterized previously [18–21].

#### *Western Blot Analysis*

Human embryonic kidney 293 (HEK-293) cells stably transfected with human sst<sub>2A</sub>, sst<sub>3</sub> or sst<sub>5</sub> as well as pituitary samples from human autopsy were lysed in detergent buffer (20 mM Hepes, pH 7.4, 150 mM NaCl, 5 mM EDTA, 1% Triton X-100, 10% glycerol, 0.1% SDS, 0.2 mM phenylmethylsulfonyl fluoride, 10 mg/ml leupeptin, 1 mg/ml pepstatin A, 1 mg/ml aprotinin, and 10 mg/ml bacitracin). Receptors were enriched using wheat germ lectin agarose beads as described previously [22]. When indicated, somatostatin receptors were deglycosylated using peptide: N-glycosidase F (PNGase F) according to the manufacturer's instructions (New England BioLabs, Beverly, Mass., USA). Samples were then subjected to 7.5% SDS polyacrylamide gel electrophoresis and immunoblotted onto PVDF membranes. Blots were incubated with the rabbit monoclonal anti-human sst<sub>3</sub> antibody UMB-5 (dilution 1:200), followed by a peroxidase-conjugated secondary anti-rabbit antibody (Santa Cruz Biotechnology, Santa Cruz, Calif., USA; dilution 1:5,000) and enhanced chemiluminescence detection (Amersham, Braunschweig, Germany).

#### *Immunocytochemistry*

Stably sst<sub>3</sub>-transfected HEK-293 cells were grown on coverslips overnight and either not exposed or exposed to 1 μM somatostatin-14 (SS-14), 1 μM octreotide or 1 μM pasireotide for 30 min (source of octreotide and pasireotide: Novartis, Basel, Switzerland). They were subsequently fixed and incubated with the rabbit monoclonal anti-human sst<sub>3</sub> antibody UMB-5 (dilution: 1:100) at 4°C overnight followed by an incubation with Alexa Fluor 488-conjugated secondary antibody (Invitrogen, Karlsruhe, Germany; dilution: 1:750). Specimens were mounted as described previously [22] and examined using a Zeiss LSM 510 Meta laser scanning confocal microscope.

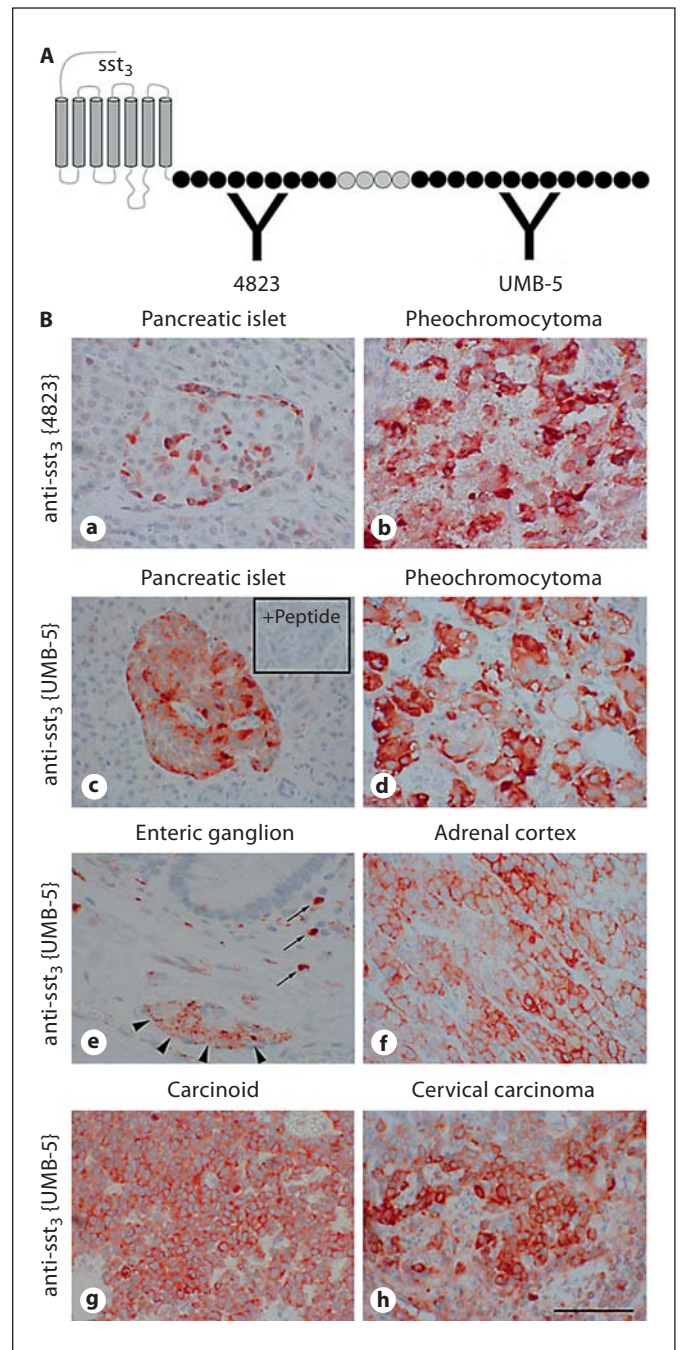
#### *Immunohistochemistry*

Five-micrometer sections were prepared from paraffin blocks and floated onto positively charged slides. Immunostaining was performed by an indirect peroxidase labeling method as described previously [23]. Briefly, sections were dewaxed, microwaved in 10 mM citric acid (pH 6.0) for 16 min at 600 W, and then incubated either with the rabbit monoclonal anti-human sst<sub>3</sub> antibody UMB-5 (dilution 1:20) or with the rabbit polyclonal anti-human sst<sub>3</sub> antibody {4823} (concentration 0.1 μg/ml), the rabbit monoclonal anti-sst<sub>2A</sub> antibody UMB-1 or the rabbit monoclonal anti-human sst<sub>5</sub> antibody UMB-4 (dilution 1:10 each) overnight at 4°C. Detection of the primary antibody was performed using a biotinylated anti-rabbit IgG followed by an incubation with peroxidase-conjugated avidin (Vector ABC 'Elite' kit, Vector Laboratories, Burlingame, Calif., USA). Binding of the primary antibody was visualized using 3-amino-9-ethylcarbazole (AEC) in acetate buffer (BioGenex, San Ramon, Calif., USA). Sections were then rinsed, counterstained with Mayer's hematoxylin and mounted in Vectamount<sup>TM</sup> mounting medium (Vector Laboratories). For immunohistochemical controls, UMB-5 was either omitted or adsorbed for 2 h at room temperature with 10 μg/ml of the peptide used for immunizations.

#### *Evaluation of the Staining Patterns*

Two independent investigators evaluated all immunohistochemical stainings. In the case of a discrepancy in the scoring between the two investigators, a final decision was achieved by

**Fig. 1.** Immunohistochemical localization of *sst*<sub>3</sub> in human normal and neoplastic tissues using the monoclonal antibody UMB-5. **A** Schematic representation of the *sst*<sub>3</sub> receptor indicating the different carboxyl-terminal epitopes of the rabbit polyclonal anti-human *sst*<sub>3</sub> antibody {4823} and the rabbit monoclonal anti-human *sst*<sub>3</sub> antibody UMB-5. **B** Sections were dewaxed, microwaved in citric acid, and incubated with either the rabbit polyclonal anti-human *sst*<sub>3</sub> antibody {4823} (**a, b**) or the rabbit monoclonal anti-human *sst*<sub>3</sub> antibody UMB-5 (**c-h**). Sections were then sequentially treated with biotinylated rabbit IgG and peroxidase-conjugated avidin. Finally, color was developed by incubation in AEC, and sections were counterstained with hematoxylin. **Inset** For adsorption controls, UMB-5 was incubated with 10 μg/ml of the peptide used for immunizations. Note that both the monoclonal antibody UMB-5 and the polyclonal antibody {4823} yielded similar staining patterns. Arrows = mast cells; arrowheads = enteric ganglion cells. Scale bar (**a-h**) = 250 μm.



consensus. All sections were scored by means of the immunoreactivity score (IRS) according to Remmele and Stegner [24], both noting the intensity of the color as well as the percentage of cells showing a positive staining. The IRS, comprising score values between 0 and 12, was calculated as follows: score [percentage of positive cells] × score [intensity of staining] = IRS; score [percentage of positive cells]: no positive cells (0); <10% (1); 10–50% (2); 51–80% (3); >80% (4); score [intensity of staining]: no staining

(0); mild (1); moderate (2); strong (3). The classification of the staining as ‘strong’ was based on the intensity of the staining of two positive control locations, pancreatic islets and pheochromocytomas (fig. 1c, d), known from the literature as strongly expressing the *sst*<sub>3</sub> receptor. Only a slight intensity of staining was classified as ‘mild’ (see, e.g., fig. 2: *sst*<sub>2</sub> expression in ACTH adenoma) and the staining intensity between ‘mild’ and ‘strong’ as ‘moderate’.



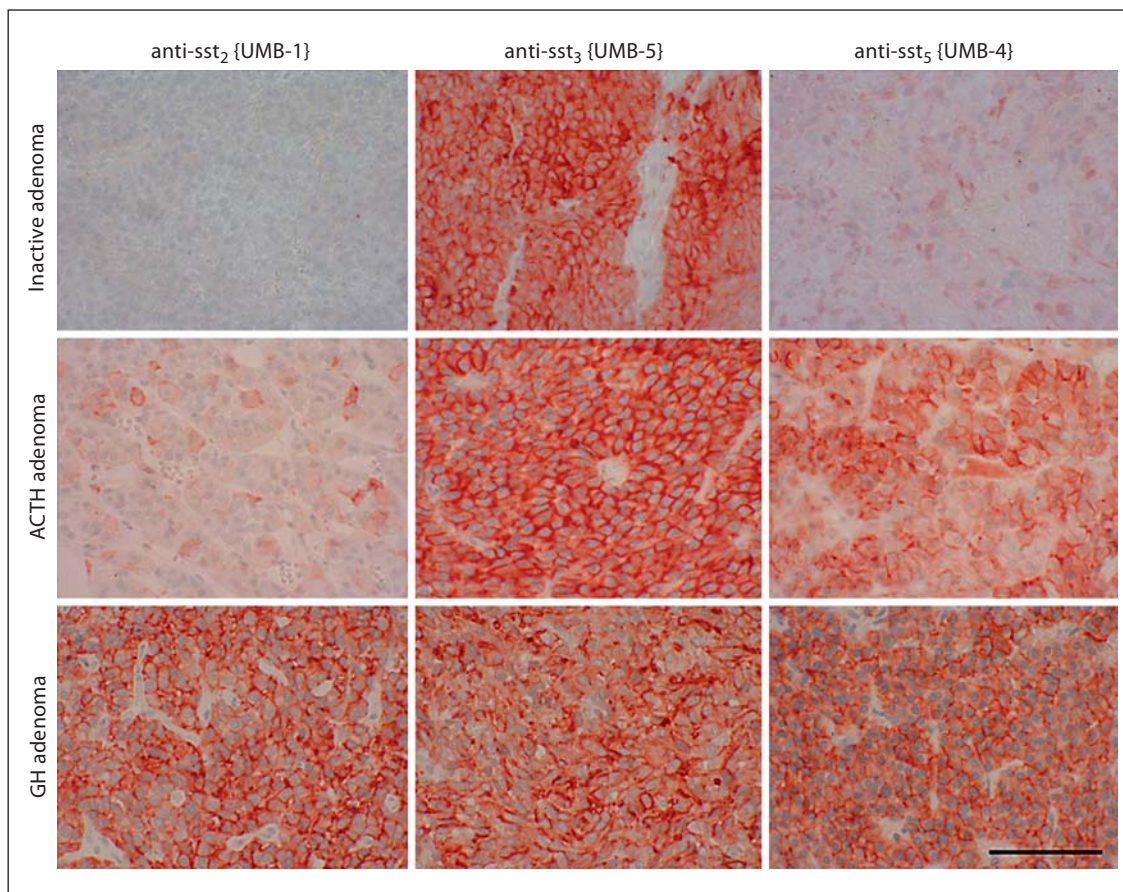


**Fig. 2.** Immunohistochemical localization of  $sst_{2A}$ ,  $sst_3$ , and  $sst_5$  in human pituitary adenomas. Sections of different types of human pituitary adenomas [non-functioning adenomas (= inactive adenomas; upper panel), ACTH-producing adenomas (middle panel), and GH-producing adenomas (lower panel)] were dewaxed, microwaved in citric acid, and incubated with either the rabbit monoclonal anti- $sst_2$  antibody UMB-1 (left panel), the rabbit monoclonal anti-human  $sst_3$  antibody UMB-5 (middle panel),

or the rabbit monoclonal anti-human  $sst_5$  antibody UMB-4 (right panel). Sections were then sequentially treated with biotinylated anti-rabbit IgG and peroxidase-conjugated avidin. Finally, color was developed by incubation in AEC, and sections were counterstained with hematoxylin. Note that, in contrast to  $sst_2$  and  $sst_5$ ,  $sst_3$  was present in all three types of human adenomas and that the immunostaining for  $sst_2$ ,  $sst_3$  as well as  $sst_5$  was predominantly localized at the plasma membrane. Scale bar = 500  $\mu\text{m}$ .

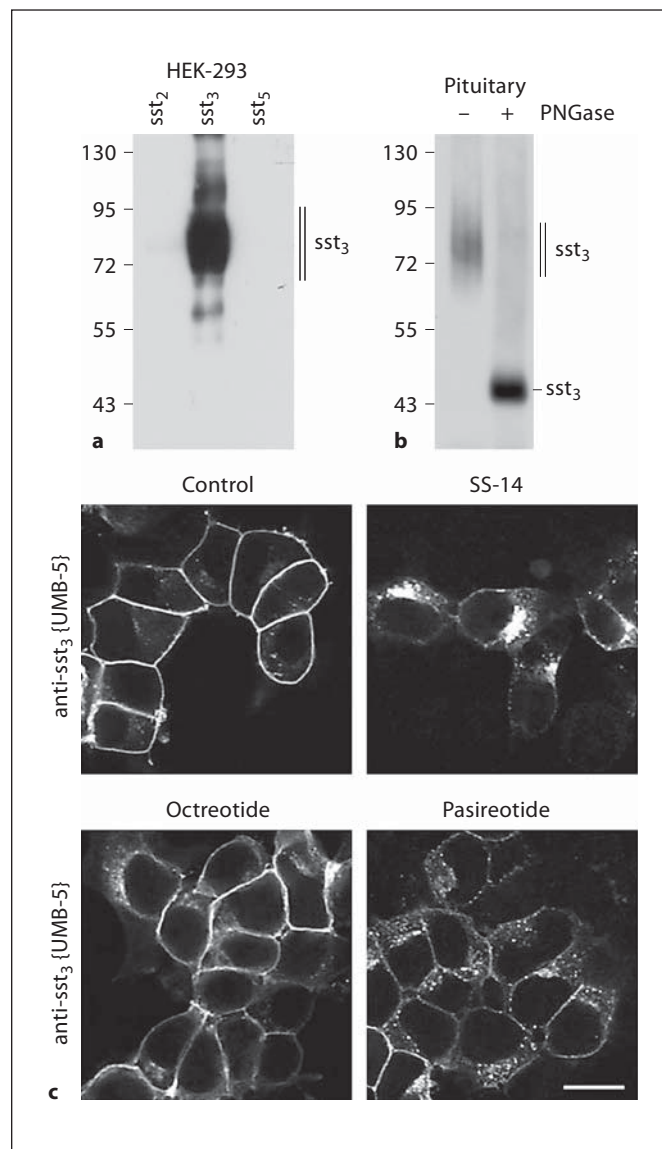
## Results

### *Characterization of the Rabbit Monoclonal Anti-Human $sst_3$ Antibody UMB-5*

The specificity of UMB-5 was initially monitored using Western blot analysis. When membrane preparations from HEK-293 cells stably transfected with human  $sst_3$ ,  $sst_{2A}$  or  $sst_5$  were electrophoretically separated and immunoblotted onto nitrocellulose, UMB-5 revealed a broad band migrating at  $M_r$  70,000–90,000 in  $sst_3$ -transfected but not in  $sst_{2A}$ - or  $sst_5$ -transfected cells (fig. 3a). UMB-5 was then characterized by immunocytochemical staining of  $sst_3$ -transfected cells. When HEK-293

cells stably expressing  $sst_3$  were stained with UMB-5, a distinct immunofluorescence localized at the level of the plasma membrane was detected (fig. 3c). Incubation with somatostatin-14 (SS-14) induced a translocation of the receptor immunoreactivity from the plasma membrane into the cytosol, indicating agonist-induced endocytosis. A similar result was obtained with pasireotide, whereas saturating concentrations of octreotide were not able to stimulate the internalization of  $sst_3$  receptors under otherwise identical conditions (fig. 3c). UMB-5 was also tested for possible cross-reactivity with other proteins present in human tissues. When membrane preparations from pituitaries from human autopsy were

**Fig. 3.** Analysis of the specificity of the monoclonal rabbit anti-human *sst*<sub>3</sub> antibody UMB-5. **a** Western blot analysis of membrane preparations from HEK-293 cells stably transfected with the human *sst*<sub>2A</sub>, *sst*<sub>3</sub> or *sst*<sub>5</sub> receptors. Samples were separated on 7.5% SDS polyacrylamide gels and blotted onto PVDF membranes. Membranes were then incubated with the rabbit monoclonal anti-human *sst*<sub>3</sub> antibody UMB-5. Blots were developed using enhanced chemiluminescence. Ordinate: migration of protein molecular weight markers ( $M_r \times 10^{-3}$ ). Note that UMB-5 selectively detected only its targeted *sst*<sub>3</sub> receptor and did not cross-react with *sst*<sub>2A</sub> or *sst*<sub>5</sub>. **b** Western blot analysis of membrane preparations from pituitaries from human autopsy. Somatostatin receptors were enriched using wheat germ lectin agarose beads and either not deglycosylated (-) or subjected to enzymatic deglycosylation using PNGase F (+). Blots were then immunoblotted with the rabbit monoclonal anti-human *sst*<sub>3</sub> antibody UMB-5 and developed using enhanced chemiluminescence. **c** Immunocytochemistry of HEK-293 cells stably transfected with the human *sst*<sub>3</sub> receptor. Cells were grown on coverslips overnight and either not exposed or exposed to 1  $\mu$ M somatostatin-14 (SS-14), 1  $\mu$ M octreotide or 1  $\mu$ M pasireotide for 30 min, subsequently fixed and immunofluorescently stained with the rabbit monoclonal anti-human *sst*<sub>3</sub> antibody UMB-5. Specimens were then examined by confocal microscopy. Representative results from one of three independent experiments are shown. Scale bar = 20  $\mu$ m.



electrophoretically separated and blotted onto PVDF membranes, UMB-5 detected a broad band migrating at  $M_r$  72,000–85,000 (fig. 3b, left panel). To test the hypothesis that the bands detected in human pituitary samples would represent the glycosylated *sst*<sub>3</sub> receptor, N-glycosylated proteins were enriched by means of lectin agarose beads and then subjected to enzymatic deglycosylation using PNGase F. In fact, after deglycosylation UMB-5 detected a distinct band migrating at  $M_r$  ~45,000, the expected molecular weight of the deglycosylated receptor (fig. 3b, right panel).

#### *Immunohistochemical Localization of sst<sub>3</sub> in Human Tumors and in Their Tissues of Origin*

The rabbit monoclonal anti-human *sst*<sub>3</sub> antibody UMB-5 was then employed for immunohistochemical stainings of a variety of human normal and neoplastic tissues. A set of tissue sections positively stained for *sst*<sub>3</sub> was also incubated with UMB-5 pre-adsorbed with the respective immunizing peptide, which in all cases led to a complete abolition of the immunostaining (see insert in fig. 1c). For comparison of the staining patterns, adjacent sections were stained with the rabbit monoclonal anti-human *sst*<sub>3</sub> antibody UMB-5 and the rabbit polyclonal anti-human *sst*<sub>3</sub> antibody {4823}, which are directed to

**Table 1.** Presence of sst<sub>3</sub> in different human tumor samples as determined by the prevalence and the immunoreactivity score (IRS) according to Remmele and Stegner [24]

Tumor type (total number of cases)	sst <sub>3</sub> positive cases, n (%)	IRS sst <sub>3</sub>		
		mean	min.	max.
Pituitary adenoma (41)	41 (100)	9.0	5	12
Non-functioning adenoma (6)	6 (100)	8	8	8
ACTH adenoma (8)	8 (100)	11.6	10	12
GH adenoma (27)	27 (100)	8.7	5	12
Glioblastoma (6)	4 (67)	2.1	0	6
Pancreatic adenocarcinoma (10)	6 (60)	1.9	0	4.5
Renal clear cell carcinoma (9)	0 (0)	0	0	0
Pheochromocytoma (13)	13 (100)	5.0	4	7.5
Neuroendocrine tumors (67)	56 (84)	4.8	0	12
of the lung (2)	2 (100)	6.0	4	8
of the gut (31)	26 (84)	4.7	0	12
Insulinoma (5)	5 (100)	7.3	4.5	8
Lymph node MTS (16)	14 (88)	5.3	0	12
Liver MTS (13)	9 (69)	3.3	0	12
Prostate adenocarcinoma (9)	0 (0)	0	0	0
Breast carcinoma (12)	4 (33)	2.7	0	12
Invasive ductal carcinoma (8)	0 (0)	0	0	0
Invasive lobular carcinoma (2)	2 (100)	5.3	4.5	6
Solid neuroendocrine carcinoma (2)	2 (100)	11.0	10	12
Cervix carcinoma (11)	4 (36)	1.7	0	6
Squamous cell carcinoma (7)	0 (0)	0	0	0
Adenocarcinoma (3)	3 (100)	4.2	3	5
Neuroendocrine tumor (1)	1 (100)	6.0	6	6
Ovarian tumors (12)	7 (58)	1.8	0	4.5
Serous-papillary adenocarcinoma (5)	1 (20)	1.8	0	4
Granulosa cell tumor (4)	3 (75)	1.8	0	4.5
Rhabdomyosarcoma (2)	2 (100)	3.5	2.5	4.5
Brenner tumor (1)	1 (100)	3.0	3	3

MTS = Metastases.

different carboxyl-terminal epitopes of the human sst<sub>3</sub> receptor. As depicted in figures 1a–d, both antibodies yielded similar staining patterns in pancreatic islets and pheochromocytomas, two previously described prominent localizations of the sst<sub>3</sub> receptor [21]. However, in many cases, the monoclonal antibody UMB-5 yielded a more distinct plasma membrane staining (fig. 1e–h). Prominent sst<sub>3</sub> immunoreactivity was found in distinct cell populations of the anterior pituitary, pancreatic islets (fig. 1c), enteric ganglion cells of the intestine (fig. 1e, arrowheads), zona fasciculata and zona reticularis of the adrenal cortex (fig. 1f) as well as in the adrenal medulla. In addition, single strongly stained round-shaped cells were observed, scattered throughout the lamina propria mucosae of the gut (fig. 1e, arrows) or throughout the stroma of various malignant tissues like renal, prostate,

breast, cervix, or ovarian tumors, probably representing mast cells.

The presence of sst<sub>3</sub> immunoreactivity in the human tumor samples investigated is summarized in table 1. Examples of typical immunostainings are shown in figure 1 and 2. In many positive cases, the immunostaining was predominantly localized at the plasma membrane of the tumor cells. However, in all sst<sub>3</sub>-expressing tumor entities investigated, not only a marked intraindividual heterogeneity, but also a huge interindividual variability both in the percentage of positive cells and in the intensity of immunostaining was noticed (table 1). Strong sst<sub>3</sub> expression was seen in all pituitary adenomas, including non-functioning, ACTH- and GH-producing adenomas (table 1; fig. 2). Interestingly, non-functioning adenomas did not exhibit any detectable or noticeable sst<sub>2A</sub> or sst<sub>5</sub>



expression (fig. 2, top panel). In the majority of the ACTH-producing adenomas, *sst*<sub>3</sub> and *sst*<sub>5</sub> were present (fig. 2, middle panel). In contrast, all GH-producing adenomas expressed *sst*<sub>3</sub> and *sst*<sub>5</sub> and in ~65% of cases *sst*<sub>2A</sub> as well (fig. 2, bottom panel). In addition, all cases of pheochromocytoma exhibited a noticeable *sst*<sub>3</sub> expression (table 1; fig. 1d). About 85% of neuroendocrine tumors and their metastases were *sst*<sub>3</sub> positive, amongst them all insulinomas (table 1; fig. 1g). The *sst*<sub>3</sub> receptor was also detectable in many glioblastomas, pancreatic adenocarcinomas, breast carcinomas (both investigated cases of invasive lobular and solid neuroendocrine carcinomas), cervix carcinomas (all cases of adenocarcinomas and the tumor with neuroendocrine differentiation) as well as ovarian tumors (table 1; fig. 1h). No immunostaining for *sst*<sub>3</sub> was observed in renal clear cell carcinomas, prostate adenocarcinomas, invasive ductal carcinomas of the breast, and squamous cell carcinomas of the cervix uteri (table 1).

## Discussion

In an effort to provide a monoclonal antibody that can be used for immunohistochemical staining of human *sst*<sub>3</sub> receptors, we extensively characterized the novel rabbit monoclonal anti-human *sst*<sub>3</sub> antibody UMB-5. We show that the very carboxyl-terminal tail of human *sst*<sub>3</sub> can serve as an epitope for the generation of a rabbit monoclonal antibody that effectively stains formalin-fixed, paraffin-embedded human tissues. There are several lines of evidence indicating that UMB-5 specifically detects its targeted receptor and does not cross-react. First, in Western blot analyses, UMB-5 selectively detected its cognate receptor and did not cross-react with other proteins present in crude extracts from *sst*<sub>2A</sub>- or *sst*<sub>3</sub>-transfected cells. Second, enzymatic deglycosylation of the receptor revealed a distinct band at a lower molecular weight, corresponding to the expected molecular weight of the deglycosylated receptor. Third, the antibody yielded a distinct staining of the cell surface of *sst*<sub>3</sub>-transfected cells. As expected from previous investigations with the polyclonal antibody {4823} [25], incubation with somatostatin-14 induced a translocation of the receptor from the plasma membrane into the cytosol, indicating agonist-induced endocytosis. A similar result was obtained with the pan-somatostatin analog pasireotide, whereas octreotide, which displays considerable lower affinity to *sst*<sub>3</sub>, was not able to cause internalization of the receptor. Fourth, UMB-5 yielded highly efficient immunostaining

of formalin-fixed, paraffin-embedded tissue samples with similar staining patterns as those observed with the polyclonal rabbit anti-human *sst*<sub>3</sub> antibody {4823}, but with more distinct plasma membrane staining. Finally, preadsorption of UMB-5 with its immunizing peptide resulted in complete abolition of immunostaining detected in tissue sections.

In normal human tissues, the rabbit monoclonal antibody UMB-5 revealed a strong staining of distinct cell populations in anterior pituitary, pancreatic islets, adrenal cortex and medulla, enteric ganglia and mast cells. The findings with respect to anterior pituitary, pancreas, and adrenal tissue are in line with previous findings obtained with polyclonal antibodies or by mRNA analysis [4, 21, 26–28]. The presence of *sst*<sub>3</sub> in enteric ganglion cells and mast cells (identified by double-labeling experiments showing the presence of mast cell protease-1 in these cells) has been recently demonstrated also by immunohistochemical investigations in the ileum of mice [29, 30].

With respect to neoplastic human tissue, the present study revealed a high prevalence of *sst*<sub>3</sub> in different types of pituitary adenoma, namely in non-functioning adenoma. Similar results have been shown previously by means of receptor autoradiography and mRNA analysis [28, 31–35]. The high prevalence of *sst*<sub>3</sub> in comparison to *sst*<sub>2</sub> and *sst*<sub>5</sub> found in the present investigation in non-functioning adenoma is also in line with clinical findings showing an insensitivity of the majority of the non-functioning adenoma to octreotide or lanreotide therapy and a higher efficacy of pasireotide treatment [33, 36–38]. In the literature, however, also contradictory results on *sst* receptor expression in non-functioning adenoma have been reported [39, 40]. These discrepancies may be related to the PCR methodology and to the antibodies (monoclonal vs. polyclonal antibodies) used in the latter investigations.

Also the high prevalence of *sst*<sub>3</sub> in pheochromocytoma and neuroendocrine tumors found in our investigations with UMB-5 corresponds well to earlier data obtained with polyclonal antibodies [4, 21, 27, 41]. In contrast to these previous investigations showing primarily cytoplasmic immunoreactivity, the present study revealed a predominance of plasma membrane staining. In accordance with data from the literature obtained with polyclonal antibodies or by means of mRNA analysis [42–46], our investigations revealed also a frequent presence of the *sst*<sub>3</sub> receptor in glioblastoma, pancreatic adenocarcinoma, and in breast, cervix uteri, and ovarian tumors.



In conclusion, we have generated and characterized a novel rabbit monoclonal anti-human sst<sub>3</sub> antibody, which enables both immunocytochemistry and immunoblotting experiments as well as the visualization of sst<sub>3</sub> receptors in human formalin-fixed, paraffin-embedded tissues during routine histopathological examinations. To our best knowledge, this is the first monoclonal anti-human sst<sub>3</sub> antibody yielding a predominance of plasma membrane staining in human tissue samples. In comparison to currently available polyclonal antibodies, the monoclonal antibody UMB-5 has the advantage that it can be produced in unlimited amounts for an unlimited time in always identical high quality. The sst<sub>3</sub> receptor was localized at a high prevalence in non-functioning and in hormonally active pituitary adenomas, in neuro-

endocrine tumors and also in different other solid neoplasms, which may open up new routes for diagnostic and therapeutic intervention, both pharmacologically and with radiolabeled sst<sub>3</sub> receptor ligands.

### Disclosure Statement

All authors declare that there is no conflict of interest that could be perceived as prejudicing the impartiality of the research reported.

### Acknowledgement

We thank Mrs Heidrun Guder for her excellent technical assistance.

### References

- 1 Corleto VD, Nasoni S, Panzuto F, Cassetta S, Delle Fave G: Somatostatin receptor subtypes: basic pharmacology and tissue distribution. *Dig Liv Dis* 2004;36(suppl 1):S8–S16.
- 2 Ben-Shlomo A, Melmed S: Pituitary somatostatin receptor signaling. *Trends Endocrinol Metab* 2010;21:123–133.
- 3 De Martino MC, Hofland LJ, Lamberts SW: Somatostatin and somatostatin receptors: from basic concepts to clinical applications. *Prog Brain Res* 2010;182:255–280.
- 4 Kulaksiz H, Eissele R, Rössler D, Schulz S, Höllt V, Cetin Y, Arnold R: Identification of somatostatin receptor subtypes 1, 2A, 3, and 5 in neuroendocrine tumours with subtype specific antibodies. *Gut* 2002;50:52–60.
- 5 Oberg KE, Reubi JC, Kwekkeboom DJ, Krenning EP: Role of somatostatins in gastroenteropancreatic neuroendocrine tumor development and therapy. *Gastroenterol* 2010;139:742–753.
- 6 Pyronnet S, Bousquet C, Najib S, Azar R, Laklai H, Susini C: Antitumor effects of somatostatin. *Mol Cell Endocrinol* 2008;286:230–237.
- 7 Msaouel P, Galanis E, Koutsilieris M: Somatostatin and somatostatin receptors: implications for neoplastic growth and cancer biology. *Expert Opin Investigat Drugs* 2009;18:1297–1316.
- 8 Lu HT, Salamon H, Horuk R: The biology and function of somatostatin receptors. *Expert Opin Ther Targets* 2001;5:613–623.
- 9 Olias G, Viollet C, Kusserow H, Epelbaum J, Meyerhof W: Regulation and function of somatostatin receptors. *J Neurochem* 2004;89:1057–1091.
- 10 Tulipano G, Schulz S: Novel insights in somatostatin receptor physiology. *Eur J Endocrinol* 2007;156:S3–S11.
- 11 Sharma K, Patel YC, Srikanth CB: Subtype-selective induction of wild-type p53 and apoptosis, but not cell cycle arrest, by human somatostatin receptor 3. *Mol Endocrinol* 1996;10:1688–1696.
- 12 War SA, Somvanshi RK, Kumar U: Somatostatin receptor-3 mediated intracellular signaling and apoptosis is regulated by its cytoplasmic terminal. *Biochim Biophys Acta* 2011;1813:390–402.
- 13 Florio T, Morini M, Villa V, Arena S, Corsaro A, Thellung S, Culler MD, Pfeffer U, Noonan DM, Schettini G, Albini A: Somatostatin inhibits tumor angiogenesis and growth via somatostatin receptor-3-mediated regulation of endothelial nitric oxide synthase and mitogen activated protein kinase activities. *Endocrinology* 2003;144:1574–1584.
- 14 Liew CW, Vockel M, Glassmeier G, Brandner JM, Fernandez-Ballester GJ, Schwarz JR, Schulz S, Buck F, Serrano L, Richter D, Kreienkamp HJ: Interaction of the human somatostatin receptor 3 with the multiple PDZ domain protein MUPP1 enables somatostatin to control permeability of epithelial tight junctions. *FEBS Lett* 2009;583:49–54.
- 15 Tulipano G, Stumm R, Pfeiffer M, Kreienkamp HJ, Höllt V, Schulz S: Differential  $\beta$ -arrestin trafficking and endosomal sorting of somatostatin receptor subtypes. *J Biol Chem* 2004;279:21374–21382.
- 16 Ginj M, Zhang H, Waser B, Cescato R, Wild D, Wang X, Ercegyi J, Rivier J, Mäcke HR, Reubi JC: Radiolabeled somatostatin receptor antagonists are preferable to agonists for in vivo peptide receptor targeting of tumors. *PNAS* 2006;103:16436–16441.
- 17 Ginj M, Zhang H, Eisenwiener KP, Wild D, Schulz S, Rink H, Cescato JC, Reubi JC, Mäcke R: New pansomatostatin ligands and their chelated versions: affinity profile, agonist activity, internalization, and tumor targeting. *Clin Cancer Res* 2008;14:2019–2027.
- 18 Fischer T, Doll C, Jacobs S, Kolodziej A, Stumm R, Schulz S: Reassessment of sst2 somatostatin receptor expression in human normal and neoplastic tissues using the novel rabbit monoclonal antibody UMB-1. *J Clin Endocrinol Metab* 2008;93:4519–4524.
- 19 Pöll F, Lehmann D, Illing S, Ginj M, Jacobs S, Lupp A, Stumm R, Schulz S: Pasireotide and octreotide stimulate distinct patterns of sst2A somatostatin receptor phosphorylation. *Mol Endocrinol* 2010;24:436–446.
- 20 Lupp A, Hunder A, Petrich A, Nagel F, Doll C, Schulz S: Reassessment of sst5 somatostatin receptor expression in normal and neoplastic human tissues using the novel rabbit monoclonal antibody UMB-4. *Neuroendocrinology* 2011;94:255–264.
- 21 Mundschenk J, Unger N, Schulz S, Höllt V, Schulz S, Steinke R, Lehnert H: Somatostatin receptor subtypes in human pheochromocytoma: subcellular expression pattern and functional relevance for octreotide scintigraphy. *J Clin Endocrinol Metab* 2001;88:5150–5157.
- 22 Schulz S, Pauli SU, Schulz S, Händel M, Dietzmann K, Firsching R, Höllt V: Immunohistochemical determination of five somatostatin receptors in meningioma reveals frequent overexpression of somatostatin receptor subtype sst2A. *Clin Cancer Res* 2000;6:1865–1874.

- 23 Lupp A, Danz M, Müller D: Morphology and cytochrome P450 isoforms expression in precision-cut rat liver slices. *Toxicol* 2001; 161:53–66.
- 24 Remmele W, Stegner HE: Recommendation for uniform definition of an immunoreactive score (IRS) for immunohistochemical estrogen receptor detection (ER-ICA) in breast cancer tissue. *Pathologe* 1987;8:138–140.
- 25 Lesche S, Lehmann D, Nagel F, Schmid HA, Schulz S: Differential effects of octreotide and pasireotide on somatostatin receptor internalization and trafficking in vitro. *J Clin Endocrinol Metab* 2009;94:654–661.
- 26 Portela-Gomes GM, Stridsberg M, Grime-lius L, Öberg K, Janson ET: Expression of five different somatostatin receptor subtypes in endocrine cells of the pancreas. *Appl Immunohistochem Mol Morphol* 2000;8:126–132.
- 27 Unger N, Serdiuk I, Sheu SY, Walz MK, Schulz S, Saeger W, Schmid KW, Mann K, Petersenn S: Immunohistochemical localization of somatostatin receptor subtypes in benign and malignant adrenal tumours. *Clin Endocrinol* 2008;68:850–857.
- 28 Nishioka H, Tamura K, Iida H, Kutsukake M, Endo A, Ikeda Y, Haraoka J: Co-expression of somatostatin receptor subtypes and estrogen receptor- $\alpha$  mRNAs by non-functioning pituitary adenomas in young patients. *Mol Cell Endocrinol* 2011;331:73–78.
- 29 Van Op den Bosch J, Van Nassauw L, Lantermann K, Van Marck E, Timmermans JP: Effect of intestinal inflammation on the cell-specific expression of somatostatin receptor subtypes in the murine ileum. *Neurogastroenterol Motil* 2007;19:596–606.
- 30 Van Op den Bosch, Lantermann K, Torfs P, Van Marck E, Van Nassauw L, Timmermans JP: Distribution and expression levels of somatostatin and somatostatin receptors in the ileum of normal and acutely *Schistosoma mansoni*-infected SSTR2 knockout/lacZ knockin mice. *Neurogastroenterol Motil* 2008;20:798–807.
- 31 Nielsen S, Mellekjaer S, Rasmussen LM, Ledet T, Olsen N, Bojsen-Moller M, Astrup J, Weeke J, Jorgensen JOL: Expression of somatostatin receptors on human pituitary adenomas in vivo and ex vivo. *J Endocrinol Invest* 2001;24:430–437.
- 32 Reubi JC, Waser B, Schaer JC, Laissue JA: Somatostatin receptor sst1–sst5 expression in normal and neoplastic human tissues using receptor autoradiography with subtype-selective ligands. *Eur J Nucl Med* 2001;28:836–846.
- 33 Taboada GF, Luque RM, Bastos W, Guimarães RFC, Marcondes JB, Chimelli LMC, Fontes R, Mata PJP, Niemeyer Filho P, Carvalho DP, Kineman RD, Gadelha MR: Quantitative analysis of somatostatin receptor subtype (SSTR1–5) gene expression levels in somatotropinomas and non-functioning pituitary adenomas. *Eur J Endocrinol* 2007; 156:65–74.
- 34 Pisarek H, Pawlikowski M, Kunert-Radek J, Radek M: Expression of somatostatin receptor subtypes in human pituitary adenomas – immunohistochemical studies. *Endokrynol Polska* 2009;60:240–251.
- 35 Tateno T, Kato M, Tani Y, Oyama K, Yamada S, Hirata Y: Differential expression of somatostatin and dopamine receptor subtype genes in adrenocorticotropin (ACTH)-secreting pituitary tumors and silent corticotroph adenomas. *Endocr J* 2009;56:579–584.
- 36 Chanson P, Brochier S: Non-functioning pituitary adenomas. *J Endocrinol Invest* 2005; 28:93–99.
- 37 Jaffe CA: Clinically non-functioning pituitary adenoma. *Pituitary* 2006;9:317–321.
- 38 Korbonits M, Carlsen E: Recent clinical and pathophysiological advances in non-functioning pituitary adenomas. *Hormone Res* 2009;71(suppl 2):123–130.
- 39 Zatelli MC, Piccin D, Vignali C, Tagliati F, Ambrosio MR, Bondanelli M, Cimino V, Bianchi A, Schmid HA, Scanarini M, Pontecorvi A, De Marinis L, Maira G, degli Uberti EC: Pasireotide, a multiple somatostatin subtypes ligand, reduces cell viability in non-functioning pituitary adenomas by inhibiting vascular endothelial growth factor secretion. *Endocr Relat Cancer* 2007;14:91–102.
- 40 Zatelli MC, Minoia M, Filieri C, Tagliati F, Buratto M, Ambrosio MR, Lapparelli M, Scanarini M, degli Uberti EC: Effect of everolimus on cell viability in nonfunctioning pituitary adenomas. *J Clin Endocrinol Metab* 2010;95:968–976.
- 41 Kaemmerer D, Peter L, Lupp A, Schulz S, Sängler J, Prasad V, Kulkarni H, Haugvik SV, Hommann M, Baum RP: Molecular imaging with 68Ga-SSTR PET/CT and correlation to immunohistochemistry of somatostatin receptors in neuroendocrine tumours. *Eur J Nucl Med Mol Imaging* 2011, DOI: [10.1007/s00259-011-1846-5](https://doi.org/10.1007/s00259-011-1846-5).
- 42 Schulz S, Schulz S, Schmitt J, Wiborny D, Schmidt H, Olbricht S, Weise W, Roessner A, Gramsch C, Höllt V: Immunocytochemical detection of somatostatin receptors sst1, sst2A, sst2B and sst3 in paraffin-embedded breast cancer tissue using subtype-specific antibodies. *Clin Cancer Res* 1998;4: 2047–2052.
- 43 Schulz S, Schmitt J, Quednow C, Roessner A, Weise W: Immunohistochemical detection of somatostatin receptors in human ovarian tumours. *Gyn Oncol* 2002;84:235–240.
- 44 Schulz S, Schmitt J, Weise W: Frequent expression of immunoreactive somatostatin receptors in cervical and endometrial cancer. *Gyn Oncol* 2003;89:385–390.
- 45 Li M, Li W, Min HJ, Yao QZ, Chen CY, Fisher WE: Characterization of somatostatin receptor expression in human pancreatic cancer using real-time RT-PCR. *J Surg Res* 2004; 119:130–137.
- 46 Mawrin C, Schulz S, Pauli SU, Treuheit T, Dietschmann K, Firsching R, Schulz S, Höllt V: Differential expression of sst1, sst2A, and sst3 somatostatin receptor proteins in low-grade and high-grade astrocytomas. *J Neuropathol Exp Neurol* 2004;63:13–19.